

## INDUSTRIAL IMPLEMENTATION OF EFFICIENCY IMPROVEMENTS IN N-TYPE SOLAR CELLS AND MODULES

I.G. Romijn<sup>1</sup>, B. van Aken<sup>1</sup>, J. Anker<sup>1</sup>, A.R. Burgers<sup>1</sup>, A. Gutjahr<sup>1</sup>, B. Heurtault<sup>1</sup>, M. Koppes<sup>1</sup>, E. Kossen<sup>1</sup>, M. Lamers<sup>1</sup>,  
D.S. Saynova<sup>1</sup>, C.J.J. Tool<sup>1</sup>

Lang Fang<sup>2</sup>, Xiong Jingfeng<sup>2</sup>, Li Gaofei<sup>2</sup>, Xu Zhuo<sup>2</sup>, Wang Hongfang<sup>2</sup>, Hu Zhiyan<sup>2</sup>

P.R. Venema<sup>3</sup>, A.H.G. Vlooswijk<sup>3</sup>

<sup>1</sup>ECN Solar Energy, P.O. Box 1, 1755 ZG Petten, The Netherlands  
Phone: +31 224 56 4309; Fax: +31 224 56 8214; email: romijn@ecn.nl

<sup>2</sup>Yingli Solar, 3399 Chaoyang North Street, Boading, China

<sup>3</sup>Tempress Systems BV, Radeweg 31, 8171 Vaassen, The Netherlands

**ABSTRACT:** This paper describes the recent developments on the n-Pasha solar cell. The n-Pasha cell is a bifacial solar cell on n-type Cz material with homogeneous diffusions and printed metallization, and is produced at an industrial scale by Yingli Solar. Until recently these cells typically reached efficiencies around 19% at both ECN and Yingli. By reducing metal coverage and improving the quality of the front side metallization, tuning the back surface field doping and improving the front and rear surface passivation, we have been able to increase the efficiency by almost 1% absolute to 20%. Reducing the metal coverage has at the same time decreased the silver consumption per cell, making the concept more cost effective. 72 n-Pasha cells with an average efficiency of 19.6% were used for a monofacial module which resulted in a module power of 334 Watt-peak.

**Keywords:** bifacial, crystalline silicon, n-type, manufacturing and processing, module integration

### 1 INTRODUCTION

At ECN, our aim is to develop high efficient, low-cost and robust solar cell and module concepts that can be easily adopted by industry. ECN has a long standing experience in developing processes for multi-crystalline p-type silicon solar cells, and implementing these in the industry. While the majority of the PV industry is still using p-type mono or multi crystalline silicon as their base material, the use of n-type mono crystalline silicon has distinct advantages.

n-type Cz material is known for its stable high lifetimes due to the absence of light induced degradation [1,2] and its higher tolerance for the most common metallic impurities like Fe [3,4]. These properties of the n-type Cz material enable very high efficient solar cells, as is shown for instance by the company Sunpower with their interdigitate back contact technology [5] and by Sharp with their hetero junction technology [6]. Both companies developed cell concepts on n-type Cz material that reach above 24% in efficiency.

In 2010 we introduced our n-type Cz-silicon solar cell concept “n-Pasha” (**P**assivated **a**ll **s**ides **H**-**p**attern) to the market together with the companies Tempress and Yingli [7]. In 2011, efficiencies of over 19% were reached with this cell concept, both at ECN and at Yingli. In 2012, the research and development on this bifacial cell and module concept has continued with targets for both efficiency improvement and cost reduction.

### 2 THE N-PASHA CELL CONCEPT

To be able to reach high efficiencies, we use a bifacial cell design on n-type Cz material. Figure 1 shows the basic configuration of our n-Pasha solar cell. The cell has an open rear side, making it suitable for bifacial applications. When these cells are put into a bifacial module light will be collected from the front as well as from the rear adding to the efficiency gain. Both front- and rear side feature H-grid metallization patterns. Yingli’s PANDA cells are based on this structure.

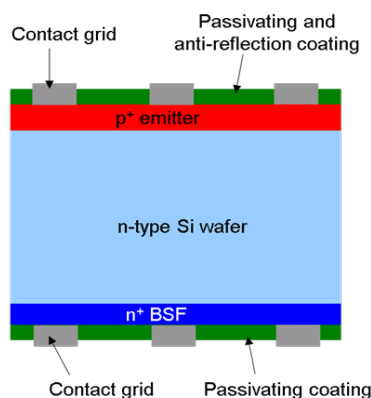


**Figure 1.** Cross section of the ECN n-pasha cell. Yingli’s PANDA cells are based on this structure.

The n-Pasha cells are fabricated on 6 inch semi-square n-type Cz wafers. The first processing step is to texture the wafers using alkaline etching resulting in a random pyramid surface structure. The boron emitter and phosphorous BSF are formed using an industrial tube furnace from Tempress [8]. A 60 ohm/sq emitter is made using  $\text{BBr}_3$  as precursor. The BSF is made using  $\text{POCl}_3$  as precursor and provides additional lateral conductivity at the rear side. This results in a good fill factor despite the open rear side metallization and in a higher tolerance to high substrate resistivities. Both the front and rear side are coated with  $\text{SiN}_x$  layers for passivating and anti-reflective purposes. The metallization is applied on both front and rear side using screen printing, and the contacts to emitter and BSF are formed during a single co-firing step in an IR-heated belt furnace. Both front and rear metallization can be directly soldered so no additional metallization step is necessary to enable stringing of the cells into a module. The open rear side also ensures that there will be no bending of the cells when (very) thin wafers are used, as is the case for the full aluminum BSF on p-type cells. All processing steps used for the n-Pasha cell are compatible with an industrial scale.

### 3 EFFICIENCY IMPROVEMENTS

#### 3.1 Starting point

During the early stages of development of n-Pasha, the main focus has been on the optimization of the boron diffusion and front surface passivation [9-11]. This resulted in average efficiencies of 19.0% in our reference 'baseline-n-Pasha' process at ECN and top efficiencies of 19.3% as reported at the previous EPVSEC in 2011 [7]. Values for  $V_{oc}$  of these n-Pasha cells were around 630 – 635 mV, depending on the material quality.

The focus in 2012 has been on improving the short-circuit current  $I_{sc}$  and open-circuit voltage  $V_{oc}$  by reducing the recombination current  $J_{0e}$  at the front and  $J_{0BSF}$  at the back of the solar cell with cost effective processes. Topics that have been investigated to lower the  $J_{0e}$  are

- Front side dielectric layer;
- Front side metal coverage;
- Passivation below metal contacts.

And to lower the recombination at the rear surface the following topics have been researched:

- BSF doping profile;
- Rear side passivation.

In the following paragraphs, the process developments leading to major improvements in cell efficiency will be highlighted.

#### 3.2 Optimizing the front side metallization

The first step toward higher efficiencies was to reduce the front Ag coverage and to reduce the recombination below the contacts.

In the past years, ECN has developed a 2-step stencil printing metallization. By the use of single layer stencil and specially developed paste, deposition of fine lines with aspect ratios of over 0.5 (height / width) was demonstrated [12]. Applying the stencil process to the n-Pasha cells, finger widths of 60  $\mu\text{m}$  have been achieved, compared to finger widths of around 100  $\mu\text{m}$  wide that were usually obtained with screen printing (see figure 2). The metal coverage of the front surface could be reduced by more than 2% absolute compared to the standard screen printing process, from approximately 7.5% to 5.5%.

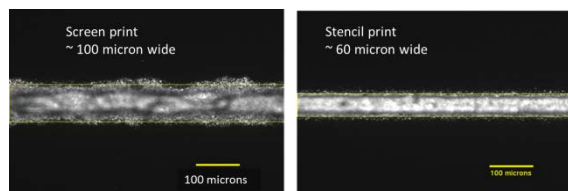


**Figure 2:** Microscope picture of a screen printed finger (left) and a stencil print finger (right)

The average  $I_{sc}$  and  $V_{oc}$  results from n-Pasha cells with a standard screen printed front side and n-Pasha cells with a stencil printed front side print are shown in figure 3. The gain in  $V_{oc}$  is mainly caused by a reduction in  $J_{0e}$ , while the gain in  $I_{sc}$  is caused by a combination of reduced metal coverage and a lower  $J_{0e}$ . The FF is around 0.5% relative lower for the stencil print due to a higher series resistance. However, this loss is more than compensated by the gain in  $I_{sc}$  and in  $V_{oc}$  resulting in an increase in efficiency of around 0.4% absolute [13].

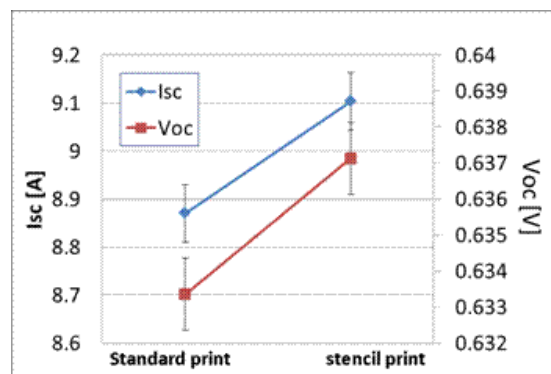


**Figure 3:** gain in  $I_{sc}$  and  $V_{oc}$  for stencil print

The front surface recombination velocity  $J_{0e}$  was further reduced by applying non-contacting busbar paste [14]. Since the three busbars of the n-pasha solar cell cover around 2.5% of the total cell area, eliminating recombination losses in this area will result in a similar or higher gain in  $V_{oc}$  as reducing the metal coverage.

Indeed, as can be seen in figure 4, a voltage gain of 4 – 6 mV is observed in experiments, with a corresponding gain in efficiency of 0.1 – 0.15% absolute.

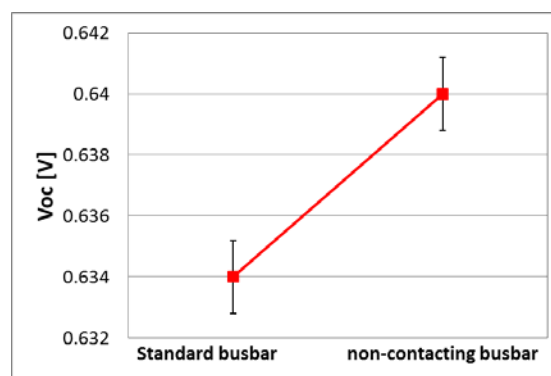


**Figure 4:** gain in  $V_{oc}$  for non-contacting busbar

Both processes described above also results in a lower silver consumption. The use of silver on the front side of n-Pasha cells has been decreased by 33%, resulting in a significant reduction in costs.

#### 3.3 Improved back surface field

The next step toward higher efficiencies of the n-Pasha cell is the improvement of the rear surface with respect to passivation and optical confinement. A lower phosphorous doping level of the BSF is expected to yield lower recombination velocities due to less Auger recombination on the one hand, and to improve the rear reflection on the other hand due to reduced free carrier absorption.

In figure 5 the implied  $V_{oc}$  values (voltage determined with QSSPC measurements on cells without metallization) are shown for cells with different BSF profiles. The sheet resistivity ( $R_{sheet}$ ) is increasing for increasing BSF number. A gain in Implied  $V_{oc}$  of ~15 mV is observed for the lowest doped BSF-3 (highest  $R_{sheet}$ ).

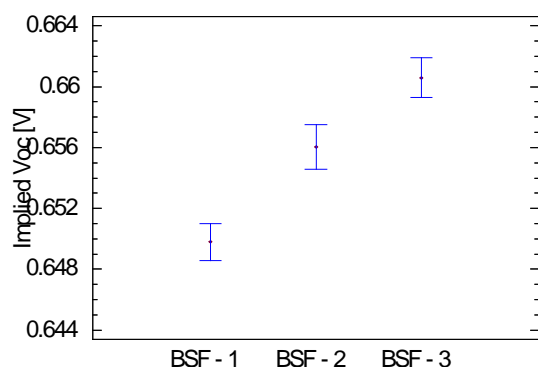


**Figure 5:** Implied  $V_{oc}$  for cells with 3 different BSF profiles with increasing sheet resistivity. ( $R_{sheet\_BSF1} < R_{sheet\_BSF2} < R_{sheet\_BSF3}$ )

On cell level, the best tested BSF doping profile was compared to the standard BSF profile on n-Cz material from different suppliers. Figure 6 shows the  $J_{sc}$  and  $V_{oc}$  data for the different n-Cz materials with base resistivity between 2 and 6 ohm-cm. For each material (distinguished by symbols) a standard group (blue symbols) and a group with improved rear surface (red symbols) was processed. The gain in  $J_{sc} * V_{oc}$  is around 3% relative, and clearly reproduced for each run, independent of the material properties.

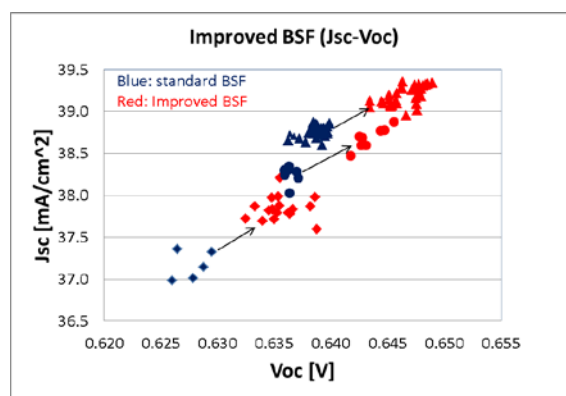


**Figure 6:** Gain in current and voltage observed in various runs using different base materials. The colors depict the type of BSF, blue for standard (BSF-1 in Figure 5) and red for improved BSF (BSF-3 in Figure 5). The symbols depict the various runs and materials used. The arrows are a guide to the eye, indicating the gain within an experiment.

For each of these experiments, a gain of 8 to 10 mV is observed for the cells with improved BSF profile, due to improved rear surface passivation. The difference in  $V_{oc}$  gain between cells with (~8-10 mV) and without metallization (15 mV) can be explained by the additional contact recombination below the metal contacts. To optimize the rear surface further, obviously reducing the metal fraction is one route. Another route is to improve the surface passivation itself by changing or adjusting the deposited dielectric layer.

Besides the gain in  $V_{oc}$ , an increase in  $J_{sc}$  is observed for the improved BSF. This is partly due to improved rear surface passivation, but is also due to a reduction in free carrier absorption. Simulations based on 2D modelling confirm the increase in  $J_{sc}$  due to both effects for lower doped BSF structures.

### 3.4 Improved passivation at front and rear surface

Lower surface doping will make the surface more sensitive to the passivation by dielectric layers. This is of course also an opportunity to improve the passivation even further. New passivation schemes have been tested for both front and rear surface. At the front side, the anti-reflective properties of the dielectric layers have also been taken into account. The gain in passivation of both front and rear side can be visualized with the internal quantum response (IQE). In figure 7, the ratio of the IQE for standard and improved front and rear surface is shown. The improved front passivation gives a gain of almost 7% in the blue wavelengths around 350 nm, while the improved rear passivation gives a gain of 2% in the red response from 900 to 1100 nm. Both improvements give rise to gains in  $I_{sc}$  and  $V_{oc}$  of around 0.5% relative but more importantly they enabled a more stable processing of large batches of n-Pasha solar cells.

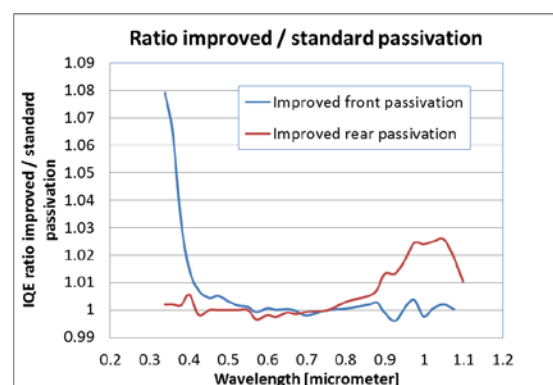


**Figure 7:** Gain in internal quantum response for improved passivation at the front (blue line) at 350 nm and at the rear (red line) between 900 and 1100 nm

### 3.5 Cell results

To reach top efficiencies, all requirements for high efficiencies need to be balanced. Lower metal coverage, lower BSF doping and good surface passivation will result in higher  $V_{oc}$  and  $J_{sc}$ . Together, the process improvements described in 3.2 to 3.4 show an increase in  $V_{oc}$  of over 20 mV. However, to maintain high FFs, especially with lower doped BSFs, two further constraints are: 1) Low contact resistance to the BSF and 2) Sufficient lateral conductance between the metal fingers to ensure high FF. We are pursuing an optimization of all these effects.

In table I, the results of cells fabricated with the newly developed processes are shown and compared to the starting point, n-Pasha cells processed with the 2011 'baseline' process (group 0). The cells processed with the 2011 'baseline-n-Pasha' process had an average efficiency of 19.0%. For the cells in group 1 the front side metallization is improved, giving an improvement in voltage and current of over 1% for both and efficiency gain of 0.4% absolute. Improving the BSF doping and surface passivation for the cells in group 2 resulted in an additional gain in both  $I_{sc}$  and  $V_{oc}$  of 1.5%. Even though the fill factor (FF) is somewhat lower for these cells, an overall efficiency gain of 0.5% absolute is realized leading to an average efficiency of 19.9%, and a highest efficiency of 20% (measured in-house, using a reflecting

measurement chuck to simulate the situation in a module)  
Compared to the n-baseline 2011, a gain in  $V_{oc}$  of 17 mV has been realized.

**Table I:** Efficiency improvements

group	Isc [A]	Voc [V]	FF [%]	Eta [%]
0:baseline	9.10	0.633	78.4	19.0
2011- avg				
1:Improved metal - avg	9.26	0.640	78.4	19.4
1:Improved metal - top	9.27	0.640	78.7	19.5
2:Improved BSF - avg	9.38	0.650	77.7	19.9
2:Improved BSF - top	9.38	0.648	78.3	20.0

#### 4 TOWARDS INDUSTRIAL PROCESSING

To test the industrial feasibility of the improved n-pasha cell concept, several test runs consisting of over 100 wafers were performed at ECN. At Yingli, some of the new processes were tested in a pilot line. The gains observed at ECN were reproduced in the industrial environment at Yingli.

Recently, two large batches of n-mono Cz wafers from different wafer suppliers have been processed at ECN into n-Pasha cells using the new “20% process”. The resistivity range of the materials in both cases was between 2 and 5.5 ohm-cm. The average and maximum values obtained with both materials are shown in table II.  $V_{oc}$  values of over 650 mV have been reached, with maximum efficiencies of 19.8% and 19.9% for these batches of material. The distribution in both  $I_{sc}$  and  $V_{oc}$  remained narrow, indicating good process stability. The main factor limiting the efficiency is the FF. For further optimization of the cell concept, the FF will be one of the main points of attention. In figure 8, the efficiency distribution for the 2 materials is shown in a histogram. In total over 300 cells have been processed with stable results.

**Table II:** Processing of large batches

	$I_{sc}$ [A]	$V_{oc}$ [V]	FF [%]	Eta [%]
<b>Material 1</b>				
> 230 cells	9.25	0.649	77.4	19.5
Best cell	9.30	0.652	78.7	19.8
<b>Material 2</b>				
> 100 cells	9.25	0.650	78.0	19.7
Best cell	9.31	0.653	78.7	19.9

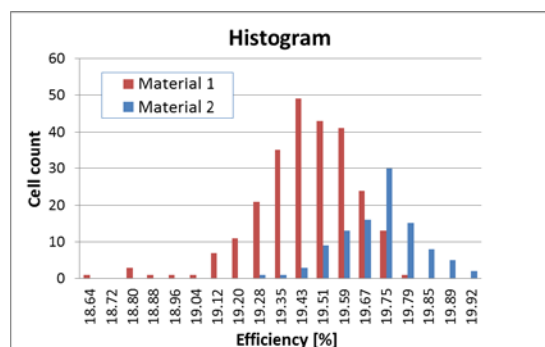


**Figure 8:** efficiency distribution for 2 materials processed with the improved n-pasha process

#### 5 N-PASHA MODULES

The >300 cells were used to manufacture monofacial and bifacial modules. Each module consists of 72 solar cells. The module results of two of them are shown in table III.

Cells with an average efficiency of 19.6% were used for the monofacial module with textured and antireflective glass (Saint-Gobain) at the front and a white TPT foil at the rear. Under standard test conditions (1000 W/m<sup>2</sup>, 25°C) this resulted in a total cell to module ratio of 98.6% and a module power of 334.3 Watt-peak.

For the bifacial module conventional textured glass was used at the front, and transparent TPT foil for the rear. For this module, cells with an average efficiency of 19.5% were used. Measurements on bifacial modules under standard test conditions (with an absorbing black plate behind the module) yield relatively low currents, since part of the light will be transmitted through the module and is not reflected at the backsheet. Under these conditions, a module output power of 315 Wp was reached. The output power of the bifacial module was also measured under conditions that are more representative for modules that are mounted in the field. Firstly, a white polystyrene board of 2 m<sup>2</sup> was put at 10 cm behind the bi-facial module. The output power increased to 331 Wp. Secondly, the wall 1.5 meter behind the module (18 m<sup>2</sup>) was covered with polystyrene boards. This way, the increase in  $I_{sc}$  yielded an output power of 376 WP, an increase of almost 20%. This demonstrates the huge possibilities for bi-facial modules, when they are placed in an appropriate way in the field. Indeed, an annual power increase of over 30% has been reported [15].

**Table III:** Results of modules

	Avg cell $\eta$ [%]	Encaps. cell $\eta$ [%]	Total area $\eta$ [%]	Power [Wp]
<b>Monofacial</b>	19.6	19.4	16.7	334
<b>Bifacial STC</b>	19.5	18.3	15.8	315
<b>PS at 10cm</b>				331
<b>PS white wall</b>				376

#### 6 SUMMARY AND CONCLUSIONS

In the past year, the main focus of the research and development of the n-Pasha solar cells has been on improving the output parameters with cost effective processes. Combined improvements of both front and rear surface have resulted in a  $V_{oc}$  gain almost 20 mV and enabled cell efficiencies of 20% on the n-Pasha solar cell. Furthermore, the reduction in metal coverage has led to a 33% reduction in front side silver consumption and therefore a cost reduction of the n-pasha cell concept. The next challenge will be to improve the FF as well as to further improve the diffusion profiles of emitter and BSF to obtain even higher efficiencies.

The newly developed processes were first tested with industrial equipment at ECN. After proof of principle and proof of concept they can be transferred to the industry at Yingli. For some of the new processes the transfer is already ongoing and efficiency gains similar to those at ECN are observed in the Panda cell line at Yingli.

We have presented a fully industrial process that resulted in 20% solar cells and over 334 Watt-peak

modules using n-Cz wafers as base material. The bifacial characteristic of the solar cell makes it possible to achieve an even higher module output power and a higher annual yield in energy.

## 7 REFERENCES

- [1] J. Schmidt et al. 26th IEEE PVSC Anaheim, 1997, p13.
- [2] S. Glunz et al., 2nd WCPEC Vienna 1998 p1343.
- [3] D. Macdonald and L.J. Geerligs, Appl. Phys. Lett. (2008) 92 p4061.
- [4] J.E. Cotter et al., 15th Workshop on Crystalline Silicon Solar Cells & Modules: Materials and Processing 2005, p3.
- [5] [us.sunpowercorp.com](http://us.sunpowercorp.com)
- [6] [www.sanyo.com/solar](http://www.sanyo.com/solar)
- [7] A.R. Burgers et al., Proc 26<sup>th</sup> EPVSEC, Hamburg, Germany, 2011
- [8] Y. Komatsu et al., Solar Energy Mat. & Solar Cells 93, 2009, p750
- [9] V.D. Mihaietchi et al., Appl. Phys. Lett., **Vol 92**, 2008, p63510
- [10] A.W. Weeber et al., Proc 24<sup>th</sup> EPVSEC, Hamburg, 2009
- [11] V.D. Mihaietchi et al., Proc. 25<sup>th</sup> EPVSEC, Valencia, Spain, 2010 p1446
- [12] B. Heurtault and J. Hoonstra, Proc 25<sup>th</sup> EPVSEC, Valencia, 2010
- [13] I.G. Romijn et al., Photovoltaics International 15, 2012, p81
- [14] M. Koenig et al., Proc 2<sup>nd</sup> Silicon PV, Leuven, 2012
- [15] L. Kreinin, et al., Proc 26<sup>th</sup> EUPVSEC, Hamburg, 2011